

Synthesis and characterization of [*trans*-di(μ -acetato)(μ -bis(diphenylphosphino)methylamine)- bis(pyridine)dimolybdenum(II)]bis(tetrafluoroborate) and derivatives

Wen-Mei Xue, Fritz E. Kühn *, Guofang Zhang, Eberhardt Herdtweck

Technical University of Munich, Institute for Inorganic Chemistry, Lichtenbergstraße 4, D-85747 Garching bei München, Germany

Received 8 August 1999; received in revised form 14 October 1999

Dedicated to Professor F. Albert Cotton on the occasion of his 70th birthday

Abstract

Reaction of *trans*-[Mo₂(μ -O₂CCH₃)₂(μ -dppma)₂(MeCN)₂](BF₄)₂ (**1**, dppma = diphenylphosphinomethylamine) with a variety of pyridine derivatives leads to axially substituted complexes of formula *trans*-[Mo₂(μ -O₂CCH₃)₂(μ -dppma)₂(NC₅H₄-R)₂](BF₄)₂ (R = H, **2**; C(CH₃)₃, **3**; C₆H₅, **4**; CH=CHC₆H₅, **5**; CCH, **6**; CN, **7**). The obtained complexes were characterized by ¹H-, ¹³C- and ³¹P{¹H}-NMR, IR, Raman spectroscopy and elemental analyses. Raman spectroscopy shows a weakening of the metal–metal interaction due to the axially coordinated pyridine ligands in all examined cases. Compound **2** was additionally examined by single-crystal X-ray analysis, revealing a Mo–Mo distance of 215.04(2) pm, which is slightly longer than that in compound **1** (213.15(3) pm). © 2000 Elsevier Science S.A. All rights reserved.

Keywords: Dimolybdenum(II); Metal–metal bonds; Pyridine derivatives; Axial ligands

1. Introduction

Many metal–metal multiply bonded complexes bearing axial ligands are known [1]. It is intriguing to explore how the formation of bonds to these axial ligands affects the length of the metal–metal bond, since the magnitude of this effect varies greatly from one species to the other. For example, for the Mo₂(O₂CR)₄-type complexes there appears to be actual resistance to the attachment of axial ligands in several cases. Especially strongly electron-withdrawing carboxylates such as O₂CCF₃ allow axial ligation, but even in this particular case the metal–axial ligand interactions are not especially strong. Dirhenium compounds also display in general only a small tendency to bind axial ligands. Interestingly, however, the analogous Cr₂(O₂CR)₄ cannot be obtained in condensed phases without them [1]. Our present interest is focused on the

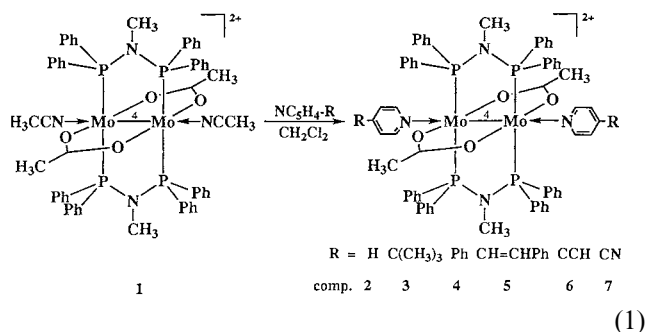
substitution reactions in the axial positions of the MoMo core, not only for the purpose of investigating the Mo–Mo and Mo–axial ligand interactions, but also to search for good building blocks bearing a MoMo core and good bridging ligands for supramolecular inorganic and organometallic materials. This field has gained considerable interest in recent years [2]. In the case of Mo(II)₂ derivatives, dimolybdenum tetracarboxylates have usually been applied as building blocks. A disadvantage of these compounds is the relatively weak interaction between the Mo(II) center and the organic ligands in the axial positions. We have recently prepared some compounds of the type *trans*-[Mo₂(μ -O₂CCH₃)₂(μ -dppma)₂(NCR)₂](BF₄)₂ where the axial ligands are nitrile derivatives [3]. The influence of the axial ligands on the MoMo moiety and the equatorial ligands is comparatively weak in those cases as well. In the present work we extend our research to pyridine derivatives and report on the preparation, structures and spectroscopic properties of the compounds of formula *trans*-[Mo₂(μ -O₂CCH₃)₂(μ -dppma)₂(NC₅H₄-R)₂](BF₄)₂. The starting material **1**, containing a dicationic

* Corresponding author.

Mo₂ unit should more easily undergo reactions with ligands such as pyridine than the neutral Mo₂(O₂CR)₄ complexes. It will be shown that the axial pyridine ligands act not only as σ -donors but also as π -acceptors, and that there is electron transfer from the equatorial ligands to the axial ones.

2. Results and discussion

Reaction of *trans*-[Mo₂(μ -O₂CCH₃)₂(μ -dppma)₂(MeCN)₂](BF₄)₂ (**1**) with a twofold stoichiometric amount of the pyridine derivatives in methylene chloride at room temperature leads to complete replacement of the acetonitrile ligands by pyridines as represented in Eq. (1). If the reaction is conducted in acetonitrile a mixture of nitrile and pyridine ligated complexes is obtained, due to the presence of the large acetonitrile excess.



Complexes **2–7** are soluble in CH₂Cl₂, CHCl₃, THF, and CH₃CN. In the last solvent the axial ligands are partially exchanged by solvent molecules (see below); in the other solvents the molecules remain unchanged.

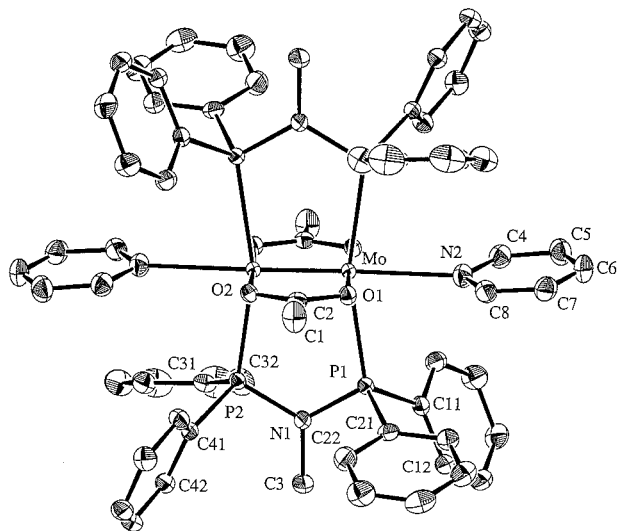


Fig. 1. ORTEP drawing of the molecular structure of the dicationic part of **2**·CH₂Cl₂. Thermal ellipsoids are at the 50% probability level. Hydrogens omitted for clarity.

Under inert gas atmosphere the complexes are stable for weeks in solution and for more than one year in solid state. However, when exposed to air they decompose within a few days in solid state and only within a couple of hours in solution.

The molecular structure of the dication in **2**·(CH₂Cl₂) is shown in Fig. 1. Selected inter atomic distances, angles and torsion angles are listed in Table 1, selected crystallographic data are presented in Table 2. Compound **2** and all other 15 crystallographically characterized structures with a *trans*-[Mo₂(μ -O₂CCH₃)₂(μ -LL)₂]²⁺

Table 1
Selected interatomic distances (pm), angles (°) and torsion angles (°) for **2**·CH₂Cl₂^a

Distances		Angles	
Mo–Mo'	215.04(2)	Mo'–Mo–N2	174.53(4)
Mo–P1	258.49(5)	Mo–N2...C6	173.83(9)
Mo–P2'	258.70(5)	P1–Mo–P2'	162.39(2)
Mo–O1	210.65(14)	O1–Mo–O2'	178.05(5)
Mo–O2'	208.79(14)	P1–N1–P2	118.11(10)
Mo–N2	259.44(18)	O1–C2–O2	121.51(17)
P1–N1	169.68(18)		
P2–N1	169.55(18)	Torsion angles	
O1–C2	126.9(2)	P1–Mo–Mo'–P2	–5.85(2)
O2–C2	127.7(2)	O1–Mo–Mo'–O2	0.23(4)
N1–C3	147.8(3)		
C2–C1	149.1(3)		

^a Translation of symmetry code to equivalent positions: (1–x, 1–y, 1–z).

Table 2
Crystallographic data for **2**·CH₂Cl₂

Chemical formula	C ₆₅ H ₆₄ B ₂ Cl ₂ F ₈ Mo ₂ N ₄ O ₄ P ₄
Formula weight	1525.48
Crystal size (mm)	0.25 × 0.13 × 0.05
Crystal system	Monoclinic
Space group	<i>P</i> 2 ₁ / <i>n</i>
<i>a</i> (pm)	1307.68(2)
<i>b</i> (pm)	1659.30(3)
<i>c</i> (pm)	1571.52(3)
β (°)	106.982(1)
<i>V</i> (10 ⁶ pm ³)	3261.3(1)
<i>Z</i>	2
ρ_{calcd} (g cm ^{–3})	1.553
μ (mm ^{–1})	0.639
<i>F</i> ₀₀₀	1548
λ (pm)	71.073
Data collected (<i>h</i> , <i>k</i> , <i>l</i>)	± 16, ± 20, ± 19
No. of parameters refined	433
<i>R</i> _{int}	0.0212
<i>R</i> ₁ ^a	0.0306
<i>wR</i> ₂ ^b	0.0667
Goodness-of-fit ^c	1.058
Weights <i>a</i> / <i>b</i> ^d	0.0148/3.6194
$\Delta\rho_{\text{max/min}}$ (e Å ^{–3})	0.59/–0.44

^a $R_1 = \Sigma(|F_o| - |F_c|) / \Sigma|F_o|$.

^b $wR_2 = [\Sigma w(F_o^2 - F_c^2)^2 / \Sigma w(F_o^2)]^{1/2}$.

^c Goodness-of-fit = $[\Sigma w(F_o^2 - F_c^2)^2 / (\text{NO} - \text{NV})]^{1/2}$.

^d $w = 1 / [\sigma^2(F_o^2) + (a^*P)^2 + b^*P]$ with $P = [\max(0 \text{ or } F_o^2) + 2F_c^2] / 3$.

type dication (LL = dppma) [4] exhibit a very similar $[\text{Mo}_2(\text{PNP})_2(\text{OCO})_2]$ core geometry. The two bridging acetates and two dppma ligands are arranged *trans* to each other. Two pyridine ligands are forced to coordinate to the molybdenum atoms in the axial positions and are slightly bent bonded. Quadruply bonded molybdenum complexes with pairs of bridging, dppa/dppma and $(\text{O}_2\text{CCH}_3)^-$ ligands usually have eclipsed conformation and occupy in the solid state a crystallographic center of inversion except for four dications, which either show a crystallographic twofold axis passing through the carbon atoms of the acetate ligands and the midpoint of the Mo–Mo bond or adapt the inversion center and the twofold axis [4c,e]. The observed Mo–Mo bond distance in **2** (215.04(2) pm) is at the upper end of the known range for Mo–Mo quadruple bonds. The Mo–O and Mo–P distances do not vary significantly for all known examples of this type. Similar as well are the P–N–P angles of the bridging dppma ligand. The P–N distances in the coordinated ligand are also very close to each other. The Mo–py bond is comparatively long (259.44(18) pm), indicating relatively weak Mo–N interaction. However, the Mo–N distance is significantly shorter than expected from the sum of the van der Waals radii (Mo–N: 382 pm) but longer than the sum of the covalent radii (Mo–N: 215 pm) [5]. The Mo–N bond distance is in length between the Mo–N interactions of $\text{Mo}_2(\text{O}_2\text{CC}(\text{CH}_3)_3)_4 \cdot \text{bipy}$ and $\text{Mo}_2(\text{O}_2\text{CCF}_3)_4 \cdot \text{bipy}$ [2].

The strong Raman bands centered around $348(\pm 5 \text{ cm}^{-1})$ can be unambiguously assigned to stretching frequencies of the Mo–Mo quadruple bond. In comparison with the axial-ligand free complex of formula $[\text{Mo}_2(\text{O}_2\text{CCH}_3)_2(\text{dppma})_2](\text{BF}_4)_2$ [$\nu(\text{Mo–Mo}) = 375 \text{ cm}^{-1}$] [3], the Mo–Mo vibration is shifted ca. 25–30 cm^{-1} to lower energies, thus indicating a weakening of the metal–metal interaction. Nitrile ligands in axial positions cause low energy shifts of about 15 cm^{-1} [3]. These observations indicate that pyridine ligands are more strongly connected to the Mo(II) centers. However, compounds **2–7** display their Mo–Mo vibration in a narrow interval of only ca. 10 cm^{-1} , a clear dependence on the donor or acceptor capability of the axial ligands cannot be seen.

In the IR spectra of complexes **2–7**, the O–C–O vibrations appear as a set of distinctive two bands at $\nu_{\text{as}}(\text{OCO}) = 1483 \text{ cm}^{-1}$ and $\nu_{\text{s}}(\text{OCO}) = 1436 \text{ cm}^{-1}$. These vibrations are located at the same energies as those of the precursor compound **1** [3].

The axial ligand 4-cyanopyridine in compound **7** contains both heterocyclic N and nitrile N atoms. Therefore it is a good tool to find out whether a coordination of the py-N atom would be preferred to a coordination of the cyano-N atom. The coordination site can be determined by comparison of the $\text{C}\equiv\text{N}$, C–C and C–N(pyridine) stretching frequencies of the free

ligand to the frequencies of complex **7**. No considerable change is observed in the $\text{C}\equiv\text{N}$ stretching of compound **7** (2239 cm^{-1}) when compared with that of 4-cyanopyridine (2243 cm^{-1}). However, the principal pyridine bands at 1594 and 1498 cm^{-1} in the free ligand are blue shifted to 1639 and 1508 cm^{-1} , respectively, in compound **7**. These features indicate the pyridine nitrogen being coordinated but the CN group being free. The Mo–Mo bond being bridged by 4-cyanopyridine is therefore excluded. A similar complex which contains 4-cyanopyridine as axial ligand for a metal–metal bonded compound, namely $[\text{Rh}_2(\text{O}_2\text{CCH}_3)_4(\text{NC}_5\text{H}_4\text{-CN})_2]$, was structurally characterized by Cotton and Felthouse [6]. In this case the ligand is also bonded to the metal center by the pyridine N. Unfortunately, crystals of the complexes **6** and **7** could only be obtained from acetonitrile–diethyl ether–*n*-hexane mixtures. Due to partial exchange of the axial ligands by solvent molecules, the crystals contain both **6** (or **7**, respectively) and **1** in an approximately 1:1 ratio.¹ However, it is clear from the obtained data that the Mo atoms are only coordinated by the pyridine N-atoms in both cases. There is also no evidence for the bridging of two MoMo cores by the axial ligands in the cases of both complexes **6** and **7**. When 4-ethynylpyridine is coordinated to the MoMo core (complex **6**), the $\text{C}\equiv\text{C}$ vibration (2112 cm^{-1}) is blue shifted from the equivalent stretching of the free ligand (2099 cm^{-1}), suggesting electron transfer from $\text{C}\equiv\text{C}$ to the pyridine ring. No evidence for bridging Mo_2 by 4-ethynylpyridine is observed in X-ray crystallography.

The proton NMR chemical shift of the CH_3CO_2 group is shifted downfield from 2.09 ppm of **1** to ca. 2.30 ppm in the cases of **2–6** and 2.34 ppm of **7**. The chemical shift of the N– CH_3 -protons of derivatives **2–7** is in the range of 2.37–2.63 ppm, which is located downfield in comparison to the equivalent resonance of **1** ($\delta(\text{H}) = 2.34 \text{ ppm}$). Among the examined complexes, 4-cyanopyridine, which contains the strongest electron-withdrawing CN group, has the strongest effect on the chemical shift of the acetate and dppma N– CH_3 protons. These facts suggest that the axial pyridine ligands are not only σ -donors but also π -acceptors. Electron transfer seems to take place from the acetate and dppma ligands through the MoMo core to the axial pyridine ligands.

Table 3 gives a comparison of the chemical shifts of the pyridine protons (H_α and H_β) in compounds **2–7**

¹ Selected crystallographic data for the **6/1** crystal mixture: monoclinic, $P2_1/n$, measurement temperature (153 \pm 1) K, $a = 1386.42(9) \text{ pm}$, $b = 1608.93(12) \text{ pm}$, $c = 1471.96(11) \text{ pm}$, $\beta = 103.133(8)^\circ$. For the **7/1** crystal mixture: monoclinic, $P2_1/n$, measurement temperature (143 \pm 1) K, $a = 1382.91(15) \text{ pm}$, $b = 1607.21(13) \text{ pm}$, $c = 1471.83(15) \text{ pm}$, $\beta = 103.069(12)^\circ$.

Table 3
Selected $^1\text{H-NMR}$ data (ppm) of the $\text{NC}_5\text{N}_4\text{-R}$ ligands in complexes 2–7^a

Complex	R	$\delta \text{H}_\alpha(\text{py})$		$\Delta\delta \text{H}_\alpha(\text{py})^b$	$\delta \text{H}_\beta(\text{py})$		$\Delta\delta \text{H}_\beta(\text{py})^b$
		Complex	Free ligand		Complex	Free ligand	
2	H	8.21(s)	8.52(m)	−0.31	7.20(t)	7.18(m)	+0.02
3	$\text{C}(\text{CH}_3)_3$	7.94(d)	8.48(q)	−0.54	7.24(d)	7.28(q)	−0.04
4	Ph	7.99(d)	8.63(q)	−0.64	7.46(d)	7.67(q)	−0.21
5	$\text{CH}=\text{CHPh}$	7.91(d)	8.55(q)	−0.64	7.24(d)	7.56(q)	−0.32
6	CCH	8.16(s)	8.56(q)	−0.40	7.15(s)	7.32(q)	−0.17
7	CN	8.71(d)	8.78(d)	−0.07	7.30(d)	7.50(d)	−0.20

^a The chemical shifts of the free ligands are given for comparison. The data were obtained in CD_2Cl_2 .

^b $\Delta\delta$, shift difference between complex and free ligand.

with the free pyridines. When coordinated, the H_α resonance is up-field shifted by 0.31–0.64 ppm in comparison to the free ligand. The only exception is derivative 7, which displays an up-field shift of only 0.07 ppm. The reason for this observation might be the back-bonding from the MoMo core to the pyridine ring because of the electron-withdrawing effect of the cyano group. H_α is deshielded due to this strong electron-withdrawing effect so that only a rather small shift is observed. The shift effect on the H_β is not as considerable as on H_α in all examined cases, although H_β shows the overall tendency of being shifted to higher field after coordination, too. Temperature-dependent $^1\text{H-NMR}$ measurement is performed on compound 7. While the temperature is lowered from +40 to -90°C , the resonances corresponding to H_α and H_β are shifted gradually to higher field from 8.74 and 7.30 ppm to 8.42 and 7.06 ppm, respectively, and the doublet signals above room temperature turn to relatively broad singlets at lower temperature. However, a dynamic exchange of the cyanopyridine ligand, especially with a coordination change between the cyano moiety and the pyridine-N atom, seems not to take place.

The $^{31}\text{P}\{^1\text{H}\}$ -NMR spectra of 2–7 display a singlet in the range 95.6–98.9 ppm since all four phosphorus nuclei are chemically equivalent. This chemical shift is comparable to that of the precursor 1 (99.7 ppm) [3] and is also similar to that of *trans*- $[\text{Mo}_2(\mu\text{-O}_2\text{CCH}_3)_2(\mu\text{-dppma})_2\text{Cl}_2]$ (100.3 ppm) [4c], implying that the axial substitution (pyridines, nitriles, halogens) has little effect on the $^{31}\text{P}\{^1\text{H}\}$ -NMR spectra.

3. Conclusions

trans- $[\text{Mo}_2(\mu\text{-O}_2\text{CCH}_3)_2(\mu\text{-dppma})_2(\text{NCCH}_3)_2](\text{BF}_4)_2$ can be easily substituted in the axial positions by pyridine derivatives. The axial ligands act not only as σ -donors but also as π -acceptors. Complexes 6 and 7, which contain $\text{C}\equiv\text{CH}$ and $\text{C}\equiv\text{N}$ moieties, seem to be potential good building blocks for organometallic and

inorganic polymers. Due to the easy and straightforward synthesis of these complexes, ligands that contain more than one pyridine function could be introduced in the axial position. In this way, one-dimensional polymers and two- and three-dimensional networks could be synthesized. In comparison with the molecules with Mo–nitrile interactions, the Mo–pyridine interactions appear to be clearly stronger as can be concluded from the Raman spectra. Substitution of the carboxylate CH_3 protons by Cl or F could lead to even stronger metal–nitrogen interactions, as it has been observed for dimolybdenum tetracarboxylates. Work in this direction is currently under way in our laboratory.

4. Experimental

4.1. General

All preparations and manipulations were carried out under an oxygen- and water-free argon atmosphere using standard Schlenk techniques. Methylene chloride was distilled over calcium hydride and diethyl ether over sodium–benzophenone, and kept over 4 Å molecular sieves. Anhydrous pyridine, *tert*-butylpyridine, benzylpyridine and 4-cyanopyridine were used as received from Aldrich. 4-Styrylpyridine [7] and 4-ethynylpyridine [8] were prepared according to references. *trans*- $[\text{Mo}_2(\mu\text{-O}_2\text{CCH}_3)_2(\mu\text{-dppma})_2(\text{MeCN})_2](\text{BF}_4)_2$ (1) was synthesized as described previously [3].

Elemental analyses were performed in the Mikroanalytisches Labor of the TU München in Garching (M. Barth). ^1H -, ^{13}C - and $^{31}\text{P}\{^1\text{H}\}$ -NMR were measured with a Bruker Avance DPX-400 spectrometer. IR spectra were obtained on a Perkin–Elmer FTIR spectrometer using KBr pellets as IR matrix. Raman spectra were measured by back scattering at room temperature (r.t.) with an instrument S.A. (Riber Jobin Yvon) model S3000 equipped with a Coherent Innova 301 Kr ion laser (647.1 nm).

4.2. Preparation of *trans*-[Mo₂(μ-O₂CCH₃)₂(μ-dppma)₂(NC₅H₄-R)₂](BF₄)₂ (R = H, **2**; C(CH₃)₃, **3**; C₆H₅, **4**; CH=CHC₆H₅, **5**; CCH, **6**; CN, **7**)

To a solution of *trans*-[Mo₂(μ-O₂CCH₃)₂(μ-dppma)₂(MeCN)₂](BF₄)₂ (**1**, 0.20 g, 0.15 mmol) in 20 ml of methylene chloride was added 0.32 mmol of the pyridine derivatives, respectively. The solution was stirred at r.t. for 4 h. After being concentrated to ca. 5 ml, the solution was treated with 20 ml of diethyl ether to precipitate a red solid. The crude product was washed with diethyl ether for a few times and then recrystallized from methylene chloride–diethyl ether. Yields are ca. 90–95%.

2: Anal. Calc. for C₆₄H₆₂B₂F₈Mo₂N₄O₄P₄ (1439.4): C, 53.36; H, 4.31; N, 3.89. Found: C, 52.98; H, 3.96; N, 4.00%. Selected IR (ν, cm⁻¹): 3052 w, 1594 m, 1482 m [asym(OCO)], 1440 vs [sym(OCO)], 1220 w, 1096 vs, 1055 vs, 998 m, 880 s, 753 m, 700 s, 669 m, 640 m, 616 w, 523 m, 500 m, 468 m. Raman (ν Mo–Mo): 345 cm⁻¹. ¹H-NMR (CD₂Cl₂, δ ppm): 2.29 (t, 6H, CH₃C), 2.49 (s, 6H, CH₃N), 7.20 (t, 4H, py-H_β), 7.31 (s, 2H, py-H_γ), 7.53–7.71 (m, 40H, Ph–H), 8.21 (s, 4H, py-H_α). ¹³C-NMR (CD₂Cl₂, δ ppm): 24.1 (CH₃C), 33.9 (CH₃N), 125.0 (py-C_β), 129.8, 132.7, 132.9, 133.0, 133.1, 133.2 (Ph–C), 139.3 (py-C_γ), 148.6 (py-C_α), 189.7 (CO₂). ³¹P{¹H}-NMR (CD₂Cl₂, δ ppm): 95.6 (s).

3: Anal. Calc. for C₇₂H₇₈B₂F₈Mo₂N₄O₄P₄ (1551.4): C, 55.69; H, 5.03; N, 3.61. Found: C, 55.26; H, 4.67; N, 3.44%. Selected IR (ν, cm⁻¹): 3055 m, 2965 m, 2869 w, 1620 s, 1483 m [asym(OCO)], 1437 vs [sym(OCO)], 1276 m, 1185 m, 1084 vs, 1066 vs, 1000 m, 969 m, 880 s, 750 m, 698 s, 670 m, 645 m, 570 m, 533 m, 500 m, 469 m. Raman (ν Mo–Mo): 350 cm⁻¹. ¹H-NMR (CD₂Cl₂, δ ppm): 1.15 (s, 18H, (CH₃)₃C), 2.30 (m, 6H, CH₃C), 2.39 (s, 6H, CH₃N), 7.24 (d, 4H, py-H_β), 7.53–7.73 (m, 40H, Ph–H), 7.94 (d, 4H, py-H_α). ¹³C-NMR (CD₂Cl₂, δ ppm): 24.8 (CH₃CO₂), 30.1 (CH₃)₃C, 34.0 (CH₃)₃C, 35.5 (CH₃N), 123.3 (py-C_β), 129.7, 129.8, 129.9, 132.9, 133.2, 133.3 (Ph–C), 149.7 (py-C_α), 166.1 (py-C_α), 190.6 (CO₂). ³¹P{¹H}-NMR (CD₂Cl₂, δ ppm): 98.9 (s).

4: Anal. Calc. for C₆₇H₆₄B₂F₈Mo₂N₄O₄P₄ (1477.4): C, 54.42; H, 4.33; N, 3.79. Found: C, 54.82; H, 4.18; N, 3.43%. Selected IR (ν, cm⁻¹): 3056 m, 1614 m, 1602 m, 1483 m [asym(OCO)], 1437 vs [sym(OCO)], 1224 w, 1188 m, 1097 vs, 1056 vs, 1000 m, 884 s, 764 m, 751 m, 700 s, 668 m, 642 m, 614 m, 526 m, 500 m, 469 m. Raman (ν Mo–Mo): 344 cm⁻¹. ¹H-NMR (CD₂Cl₂, δ ppm): 2.30 (m, 6H, CH₃C), 2.59 (s, 6H, CH₃N), 7.46 (d, 4H, py-H_β), 7.51–7.70 (m, 50H, Ph–H), 7.99 (d, 4H, py-H_α). ¹³C-NMR (CD₂Cl₂, δ ppm): 24.5 (CH₃C), 34.0 (CH₃N), 122.2 (py-C_β), 127.3, 129.5, 129.6, 129.9, 130.8, 133.0, 133.1, 133.2, 136.8 (Ph–C), 149.8 (py-C_α), 151.1 (py-C_γ), 190.0 (CO₂). ³¹P{¹H}-NMR (CD₂Cl₂, δ ppm): 95.6 (s).

5: Anal. Calc. for C₈₀H₇₄B₂F₈Mo₂N₄O₄P₄ (1643.4): C, 58.42; H, 4.50; N, 3.41. Found: C, 58.30; H, 4.31; N, 3.14%. Selected IR (ν, cm⁻¹): 3056 m, 1602 s, 1482 m [asym(OCO)], 1436 vs [sym(OCO)], 1188 m, 1098 vs, 1061 vs, 999 m, 882 s, 815 m, 749 s, 696 vs, 669 m, 642 m, 527 s, 500 m, 470 m. Raman (ν Mo–Mo): 347 cm⁻¹. ¹H-NMR (CD₂Cl₂, δ ppm): 2.30 (m, 6H, CH₃C), 2.57 (s, 6H, CH₃N), 6.93 (s, 2H, PhCH), 6.97 (s, 2H, pyCH), 7.24 (d, 4H, py-H_β), 7.34–7.74 (m, 50H, Ph–H), 7.91 (d, 4H, py-H_α). ¹³C-NMR (CD₂Cl₂, δ ppm): 24.5 (CH₃C), 33.9 (CH₃N), 121.8 (py-C_β), 124.5, 127.8, 129.3, 129.8, 130.0, 133.0, 133.1, 133.2, 135.7 (PhCH), 136.9 (pyCH), 148.5 (py-C_α), 149.0 (py-C_γ), 189.9 (CO₂). ³¹P{¹H}-NMR (CD₂Cl₂, δ ppm): 95.6 (s).

6: Anal. Calc. for C₆₈H₆₂B₂F₈Mo₂N₄O₄P₄ (1487.4): C, 54.86; H, 4.17; N, 3.77. Found: C, 54.79; H, 4.26; N, 3.45%. Selected IR (ν, cm⁻¹): 3293 m (CC–H), 3056 m, 2112 w (C≡C), 1598 s, 1483 m [asym(OCO)], 1436 vs [sym(OCO)], 1188 m, 1098 vs, 1061 vs, 998 m, 888 s, 849 w, 752 m, 700 s, 668 m, 641 s, 525 s, 500 m, 470 s. Raman (ν Mo–Mo): 349 cm⁻¹. ¹H-NMR (CD₂Cl₂, δ ppm): 2.31 (s, 6H, CH₃C), 2.37 (s, 6H, CH₃N), 3.39 (s, 2H, CCH), 7.15 (s, 4H, py-H_β), 7.38–7.66 (m, 40H, Ph–H), 8.16 (s, 4H, py-H_α). ¹³C-NMR (CD₂Cl₂, δ ppm): 24.0 (CH₃C), 30.1 (CH₃N), 66.0 (CCH), 126.5 (py-C_β), 129.3, 129.7, 130.3, 131.3, 132.3, 132.6, 132.8, 133.0, 133.3 (Ph–C and py-C_γ), 150.3 (py-C_α), 189.0 (CO₂). ³¹P{¹H}-NMR (CD₂Cl₂, δ ppm): 98.9 (s).

7: Anal. Calc. for C₆₆H₆₀B₂F₈Mo₂N₆O₄P₄ (1489.4): C, 53.18; H, 4.03; N, 5.64. Found: C, 53.39; H, 4.18; N, 5.32%. Selected IR (ν, cm⁻¹): 3049 w, 2932 w, 2239 w (C≡N), 1639 s, 1600 m, 1508 m, 1482 m [asym(OCO)], 1436 vs [sym(OCO)], 1189 w, 1098 vs, 1083 vs, 1059 vs, 1000 m, 889 s, 748 s, 699 s, 668 m, 642 m, 524 s, 498 m, 472 m. Raman (ν Mo–Mo): 353 cm⁻¹. ¹H-NMR (CD₂Cl₂, δ ppm): 2.34 (t, 6H, CH₃C), 2.63 (s, 6H, CH₃N), 7.30 (d, 4H, py-H_β), 7.37–7.66 (m, 40H, Ph–H), 8.71 (d, 4H, py-H_α). ¹³C-NMR (CD₂Cl₂, δ ppm): 23.9 (CH₃C), 31.0 (CH₃N), 116.8 (CN), 124.3 (py-C_γ), 125.6 (py-C_β), 128.6, 129.6, 132.5, 132.7, 133.1, 133.4 (Ph–C), 151.1 (py-C_α), 189.2 (CO₂). ³¹P{¹H}-NMR (CD₂Cl₂, δ ppm): 98.9 (s).

4.3. X-ray data collection, structure solution and refinement for the complex **2**·CH₂Cl₂

Suitable single crystals for the X-ray diffraction studies were grown by diffusion of diethyl ether into a methylene chloride solution of **2** at r.t. The structure was solved by a combination of the Patterson method and difference-Fourier syntheses. Full-matrix least-squares refinements were carried out by minimizing Σw(F_o² – F_c²)² with the SHELXL-97 weighting scheme and stopped at shift/err < 0.001. Neutral atom scattering factors for all atoms and anomalous dispersion corrections for the non-hydrogen atoms were taken

from the *International Tables for X-Ray Crystallography* [9a]. Preliminary examination and data collection were carried out on a four-circle Diffractometer (Nonius Mach3) equipped with an area detecting system (Nonius Kappa-CCD), a rotating anode (Nonius FR591; 50 kV; 80 mA; 4.0 kW), and graphite monochromated Mo-K α radiation. Data collection was performed at 153 K within the θ -range of $2.17 < \theta < 26.36^\circ$. A total of 27 291 reflections was collected and scaled; systematic absent reflections were rejected from the original data set. After merging, a sum of 6624 independent reflections remained and was used for all calculations. Data were corrected for Lorentz and polarization effects [9b]. All non-hydrogen atoms of the asymmetric unit were refined anisotropically. Hydrogen atoms were calculated in ideal positions (riding model; $U_H = 1.2/1.5 \times U_C$). The unit cell parameters were obtained by full-matrix least-squares refinements of 14 915 reflections with the program DENZO-SMN.

All calculations were performed on a DEC 3000 AXP workstation and an Intel Pentium II PC, with the STRUX-V [9c] system, including the programs PLATON [4], SIR92 [9d], and SHELXL-97 [9e]. A summary of the crystal and experimental data is reported in Table 2.

5. Supplementary material

Crystallographic data (excluding structure factors) for the structure reported in this paper have been deposited with the Cambridge Crystallographic Data Center as supplementary publications, CCDC No. 135415. Copies of the data can be obtained free of charge on application to CCDC, 12 Union Road, Cambridge CB2 1EZ, UK (fax: +44-1223-336033; e-mail: deposit@ccdc.cam.ac.uk).

Acknowledgements

W.-M.X. thanks the Alexander von Humboldt Foundation for a fellowship as a postdoctoral research associate, and G.Z. the Katholischer Akademischer Ausländer-Dienst for a stipend. Professor W.A. Herr-

mann is acknowledged for continuous support of our work and Dr G. Raudaschl-Sieber for experimental assistance in Raman spectroscopy.

References

- [1] F.A. Cotton, R.A. Walton, *Multiple Bonds between Metal Atoms*, 2nd edition, Oxford University Press, London, 1993, and Refs. cited therein.
- [2] (a) M. Handa, H. Matsumoto, D. Yoshioka, R. Nukada, M. Mikuriya, I. Hiromitsu, K. Kasuga, *Bull. Chem. Soc. Jpn.* 71 (1998) 1811. (b) M. Handa, M. Mikuriya, T. Kotera, K. Yamada, T. Nakao, H. Matsumoto, K. Kasuga, *Bull. Chem. Soc. Jpn.* 68 (1995) 2567. (c) X. Ouyang, C. Campana, K.R. Dunbar, *Inorg. Chem.* 35 (1996) 7188. (d) M. Handa, H. Matsumoto, T. Namura, T. Nagaoka, K. Kasuga, M. Mikuriya, T. Kotera, R. Nukada, *Chem. Lett.* (1995) 903. (e) F.A. Cotton, Y. Kim, J. Lu, *Inorg. Chim. Acta* 221 (1994) 1. (f) M. Handa, M. Mikuriya, R. Nukada, H. Matsumoto, K. Kasuga, *Bull. Chem. Soc. Jpn.* 67 (1994) 3125. (g) F.A. Cotton, Y. Kim *J. Am. Chem. Soc.* 115 (1993) 8511. (h) M. Handa, K. Yamada, T. Nakao, K. Kasuga, M. Mikuriya, T. Kotera, *Chem. Lett.* (1993) 1969. (i) M. Handa, K. Kasamatsu, K. Kasuga, M. Mikuriya, T. Fujii, *Chem. Lett.* (1990) 1753. (j) M.C. Kerby, B.W. Eichorn, J.A. Creighton, K.P.C. Vollhardt, *Inorg. Chem.* 29 (1990) 1319.
- [3] W.-M. Xue, F.E. Kühn, G. Zhang, E. Herdtweck, G. Raudaschl-Sieber, *J. Chem. Soc. Dalton Trans.* 22 (1999) 4103.
- [4] (a) Y.-Y. Wu, J.-D. Chen, L.-S. Liuo, J.-C. Wang, *Inorg. Chim. Acta* 258 (1997) 193. (b) F.A. Cotton, F.E. Kühn, *Inorg. Chim. Acta* 252 (1996) 257. (c) F.A. Cotton, F.E. Kühn, A. Yokochi, *Inorg. Chim. Acta* 252 (1996) 251. (d) D.I. Arnold, F.A. Cotton, F.E. Kühn, *Inorg. Chem.* 35 (1996) 4733.
- [5] A.L. Spek, *Platon, A Multipurpose Crystallographic Tool*, Utrecht University, Utrecht, The Netherlands, 1999.
- [6] F.A. Cotton, T.R. Felthouse, *Acta Crystallogr.* C40 (1984) 42.
- [7] M.-C. Chiang, W.H. Hartung, *J. Org. Chem.* 10 (1945) 21.
- [8] L.D. Ciana, A. Haim, *J. Heterocyclic Chem.* 21 (1984) 607.
- [9] (a) A.J.C. Wilson (Ed.), *International Tables for Crystallography*, Vol. C, Kluwer Academic Publishers, Dordrecht, The Netherlands, 1992, Table 6.1.1.4, pp. 500–502, 4.2.6.8, pp. 219–222, and 4.2.4.2, pp. 193–199. (b) Z. Otwinowski, W. Minor, *Processing of X-ray diffraction data collected in oscillation mode*, in: W.C. Carter Jr., R.M. Sweet (Eds.), *Methods in Enzymology*, USA, Academic Press, 1996, p. 276. (c) G. Artus, W. Scherer, T. Priermeier, E. Herdtweck, *Strux-V, A Program System to Handle X-Ray Data*, TU München, Germany, 1997. (d) A. Altomare, G. Cascarano, C. Giacovazzo, A. Guagliardi, M.C. Burla, G. Polidori, M. Camalli, SIR92, *J. Appl. Crystallogr.* 27 (1994) 435. (e) G.M. Sheldrick, SHELXL-97, University of Göttingen, Göttingen, Germany, 1998.